Frontiers in Bioscience Landmark

Front. Biosci. (Landmark Ed) **2025**; 30(4): 37810
https://doi.org/10.31083/FBL37810

Original Research

VSIG4 Alleviates Intracranial Hemorrhage Injury by Regulating Oxidative Stress and Neuroinflammation in Macrophages via the NRF2/HO-1 Signaling Pathway

Haofan Lu[1,2,†], Yuntao Li[1,2,†], Yonggang Zhang[1], Wen Qin[3], Zhongzhou Su[1], Sheng Qiu[1,2,*], Lifang Zheng[4,*]

[1]Department of Neurosurgery, Fifth School of Clinical Medicine of Zhejiang Chinese Medical University (Huzhou Central Hospital), 313000 Huzhou, Zhejiang, China
[2]Department of Neurosurgery, Huzhou Key Laboratory of Basic Research and Clinical Translation for Neuromodulation, 313000 Huzhou, Zhejiang, China
[3]College of Pharmacy, Shenzhen Technology University, 518118 Shenzhen, Guangdong, China
[4]Department of Neurology, Southern University of Sciences and Technology Yantian Hospital, 518081 Shenzhen, Guangdong, China
*Correspondence: qius2001@126.com (Sheng Qiu); zlf027@163.com (Lifang Zheng)
[†]These authors contributed equally.
Academic Editor: Lin-Hua Jiang
Submitted: 9 February 2025 Revised: 18 March 2025 Accepted: 31 March 2025 Published: 22 April 2025

Abstract

Background: Oxidative stress and neuroinflammation are important secondary injury mechanisms in intracranial hemorrhage (ICH). V-set and immunoglobulin domain-containing 4 (VSIG4) has an inhibitory effect on oxidative stress and the inflammatory response. This study aimed to explore the possible role of VSIG4 in ICH-related neuropathology. **Methods**: In this study, VSIG4 levels were investigated in an ICH mouse model and lipopolysaccharide (LPS)-stimulated RAW264.7 cells. Moreover, we examined oxidative stress levels, pro-inflammatory cytokine production, neuronal damage, inflammatory cell activation, brain water content, and neurological function. We performed these assays in ICH mice and macrophages with different VSIG4 levels. Additionally, the critical role of the nuclear factor erythroid 2 related factor 2/heme oxygenase-1 (NRF2/HO-1) signaling pathway in VSIG4 function was verified. **Results**: VSIG4 ameliorated neurological deficits in ICH mice ($p < 0.01$), alleviated cerebral edema ($p < 0.05$), and increased glutathione ($p < 0.05$) and decreased superoxide dismutase (SOD) levels ($p < 0.01$) in the perihematomal area and LPS-stimulated RAW264.7 cells. It also reduced Malondialdehyde (MDA) accumulation ($p < 0.01$), alleviated oxidative stress, and decreased interleukin-1β (IL-1β) ($p < 0.01$) and tumor necrosis factor-alpha (TNF-α) levels ($p < 0.01$), thereby attenuating the inflammatory response. Additionally, treatment of LPS-stimulated RAW264.7 cells with VSIG4 resulted in less damage to HT22 cells ($p < 0.05$). To further validate the involvement of the NRF2/HO-1 pathway in VSIG4-mediated neuroprotection, brusatol (an NRF2 inhibitor) was administered. **Conclusion**: Our study demonstrates the neuroprotective effect and mechanism of action of VSIG4 in ICH.

Keywords: intracranial hemorrhage; NRF2/HO-1 signaling pathway; VSIG4; neuroinflammation; oxidative stress

1. Introduction

Intracranial hemorrhage (ICH) is a significant global health burden and a leading cause of disability and mortality [1]. The severity of ICH is attributed to its complex pathophysiological mechanism, which involves both direct and secondary injuries [2]. The former mainly results from the mechanical compression of the hematoma on brain tissue and subsequent tissue necrosis caused by ischemia and hypoxia. The latter includes cascading effects such as neuroinflammation, oxidative stress, calcium overload, ferroptosis, and blood-brain barrier disruption [2,3]. Although direct damage caused by ICH can be alleviated with appropriate neurosurgical treatment, effective treatment options for secondary injury mechanisms remain limited [4]. However, secondary injuries are key factors affecting patient prognosis [5,6]. This presents a significant challenge for ICH treatment strategies. Therefore, it is imperative to conduct comprehensive research on the potential mechanisms of secondary damage following ICH. This will facilitate the development of new treatments in the future, thereby enhancing patient recovery and quality of life.

V-set and immunoglobulin domain-containing 4 (VSIG4) represents a novel class of immunomodulatory proteins predominantly expressed on the cell membrane of tissue-resident macrophages. It can inhibit excessive immune responses by suppressing the complement pathway, regulating macrophages, and influencing T cells [7–9]. In previous studies, VSIG4 was found to alleviate the progression of hepatitis, inflammatory bowel disease, and myocardial infarction by inhibiting inflammatory responses and oxidative stress [10–12]. In central nervous system diseases, Parkinson's disease and ischemic stroke can also benefit from high VSIG4 expression levels [13,14]. Furthermore, it has been suggested that the protective effect

of VSIG4 may be achieved by increasing nuclear factor erythroid 2 related factor 2 (NRF2) expression and promoting its translocation [15]. Neuroinflammation and oxidative stress are important forms of secondary injury after ICH and have a significant impact on patient prognosis [16,17]. Based on these findings, VSIG4 likely mitigates ICH-induced secondary damage through dual anti-inflammatory and antioxidant mechanisms within the central nervous system. Nevertheless, the precise mechanistic role of VSIG4 in ICH pathogenesis is yet to be fully elucidated.

In this study, we investigated the function of VSIG4 in the regulation of ICH injury. Understanding this mechanism may provide new insights into potential therapeutic targets, ultimately enhancing patient recovery and improving the prognosis associated with secondary ICH injury.

2. Materials and Methods

2.1 Animals

Male C57BL/6 mice (8–10 weeks old, 22–25 g) were sourced from Shanghai Laboratory Animal Center and acclimatized for 7 days at Huzhou Central Hospital's Animal Experiment Center before surgical procedures. The animal room is a barrier environment for specific pathogens (SPF) with a temperature controlled at 20–26 °C, relative humidity of 40%–70%, and a 12-hour light/dark cycle. The mice were housed in polycarbonate cages with 3–5 mice per cage, with a heat-sterilized bedding material at the bottom, which was replaced twice a week. The laboratory animals had free access to standard autoclaved laboratory mouse feed and sterile drinking water. All animal experiments complied with institutional ethical guidelines approved by the hospital's Animal Care Committee (Approved number: 202411005).

2.2 Cell Culture

RAW264.7 and HT22 cells were obtained from Central Laboratory of Huzhou Hospital (Huzhou, China). Cells were cultured in DMEM (Gibco, 11965, Waltham, MA, USA) supplemented with 10% heat-inactivated FBS (Gibco, A3161002) and 1% penicillin-streptomycin (Gibco, 15140122) to ensure optimal growth. The cells were incubated at 37 °C in a 5% CO_2 atmosphere. All cell lines underwent short tandem repeat profiling for authentication and tested negative for Mycoplasma.

2.3 Study Design

2.3.1 Expression Profiling of VSIG4 in ICH Pathology

An ICH model was established in 10 mice, with cohorts euthanized (See section 2.11 for euthanasia methods) at 1-day (n = 6) and 3-day (n = 6) post-operation for behavioral assessment (neurological deficit scoring) and brain tissue collection. *In vitro*, RAW264.7 macrophages were stimulated with lipopolysaccharide (LPS) (1 µg/mL) for 6, 12, or 24 hours to model ICH-associated inflammation, with untreated cells as controls.

2.3.2 Therapeutic Evaluation of VSIG4 in ICH

45 ICH model mice were randomized into three treatment groups (n = 15/group): Vehicle (PBS, intraventricular), Isotype IgG (10 mg/kg, intraventricular), Recombinant VSIG4 (5 mg/kg, intraventricular). For *in vitro* validation, RAW264.7-HT22 co-cultures received: IgG (1 µg/mL), VSIG4 (100 µg/mL), LPS + IgG, LPS + VSIG4.

2.3.3 Brusatol-Mediated Modulation of VSIG4 Efficacy

60 Mice were allocated to four cohorts (n = 15/group): ICH, ICH + Brusatol (1 mg/kg, intraventricular), ICH + VSIG4, ICH + Brusatol + VSIG4. Parallel *in vitro* experiments subjected LPS-stimulated RAW264.7 cells to: LPS, LPS + Brusatol (10 µg/mL), LPS + VSIG4, LPS + Brusatol + VSIG4.

2.4 ICH Model Building

The mice were anesthetized using a 2% isoflurane/air mixture in a general-purpose small animal anesthesia machine (RWD R500, Shenzhen, China) before being placed on a stereotaxic apparatus. After drilling a hole in the skull, a 32-gauge needle was inserted into the right striatum using coordinates of 2.0 mm from the median line, 1.0 mm from the bregma, and a depth of insertion of 4.0 mm below the brain's surface. Autologous whole blood (obtained from the caudal vein) was injected into each mouse over 10 min using a microsyringe. After injection, the needle was left in place for 5 minutes to prevent blood reflux before being gently withdrawn. The wound was then sutured. The overall generation rate of mice within 72 h post-ICH was approximately 85%, and mice with a modified Neurological Severity Score (mNSS) greater than 2 were considered successfully modeled. The mice in the sham-operated group underwent the same procedure, except that no blood was injected.

2.5 Cell Viability Assay

Cell viability was assessed via the Cell Counting Kit-8 (CCK8) assay (Sigma-Aldrich, 96992, St. Louis, MO, USA) in accordance with the supplier's standardized protocol.

2.6 Measurement of Superoxide Dismutase (SOD), Malondialdehyde (MDA), and Glutathione (GSH)

We used Beyotime assay kits to measure various biochemical activities: a Superoxide Dismutase Assay Kit (Beyotime, S0101S, Shanghai, China) for SOD activity, Lipid Peroxidation MDA Assay Kit (Beyotime, S0131S, Shanghai, China) for MDA levels, and Micro Reduced Glutathione Assay Kit (Beyotime, S0053, Shanghai, China) for GSH measurement. All experimental steps were executed as specified in the manufacturer's guidelines.

2.7 Western Blot

After treatment, tissues and cells were lysed using a radioimmunoprecipitation assay-based solution containing protease inhibitors. Extracted proteins were resolved by SDS-polyacrylamide gel electrophoresis, transmitted to a polyvinylidene difluoride membrane, blocked with FBS, and cleared with PBS. Subsequently, the membrane was incubated overnight at 4 °C with primary antibodies, namely rabbit anti-mouse NRF2 (1:2000; CST, 12721, Danvers, MA, USA), heme oxygenase-1 (HO-1) (1:2000; CST, 70081, USA), B-cell lymphoma 2 (Bcl-2) (1:2000; CST, 3498, USA), Bax (1:2000; CST, 2772, USA), VSIG4 (1:2000; Abcam, ab252933, Cambridge, UK), and GAPDH (1:2000; CST, 2118, USA). After three 5-minute wash cycles with PBS, the substrate was coupled to a goat anti-rabbit IgG horseradish peroxidase secondary antibody (1:3000; Affinity, S0001, USA) for 1 hour at room temperature. Protein signals were visualized using an enhanced chemiluminescence system and quantified via scanning densitometry and computer-aided image analysis. Protein levels were reported as the ratio of each detected band to that of GAPDH.

2.8 Reverse Transcription Quantitative (RT-q) PCR

RNA isolation from tissue and cell samples was carried out with TRIzol reagent per the manufacturer's protocol, followed by reverse transcription of RNA into cDNA using commercial kits. RT-qPCR was performed using a specific PCR system according to the manufacturer's instructions. The PCR cycling conditions consisted of the following steps: The initial step was a pre-denaturation phase, which was performed at 95 °C for 10 min. After that, 40 cycles were carried out. Each cycle involved denaturation at 95 °C for 15 s and then an annealing and extension phase at 60 °C for 35 s. PCR was performed in triplicate for each sample. Each experiment was repeated at least three times. Data were analyzed using the comparative CT ($\Delta\Delta$CT) method to calculate relative gene expression levels. The following primer sequences were used: VSIG4 (F-CCTGGGCCACCTAATAGTGC, R-TGTAGCCTCTCAGGGGATCAT), GAPDH (F-TTGTCATGGGAGTGAACGAGA, R-CAGGCAGTTGGTGGTACAGG).

2.9 ELISA

The interleukin-1β (IL-1β) (Epizyme, HJ177, Shanghai, China) and tumor necrosis factor-alpha (TNF-α) (Epizyme, HJ207, Shanghai, China) ELISA kits were obtained from Epizyme. The concentrations of these molecules were determined using ELISA kits, following the manufacturer's guidelines.

2.10 Neurological Score

Three days post-ICH, the mice were evaluated using the mNSS as described [18,19]. The scoring scale ranged from 0 (no visible neurological impairment) to 18 (the most severe neurological impairment). The mNSS assesses motor function, sensory responses, balance, and reflexes. Motor deficits, sensory impairments, balance dysfunction, and reflex abnormalities were scored on a scale of 0–6, 0–2, 0–6, and 0–4, respectively. All evaluations were conducted by trained investigators who were blinded to the experimental groups.

2.11 Evaluation of Brain Water Content

72 h after ICH, the mice were sacrificed by cervical dislocation. Immediately thereafter, the brain specimens were divided into four parts: the ipsilateral cortex (Ipsi-CX), basal ganglia on the ipsilateral side (Ipsi-BG), contralateral cortex (Cont-CX), and basal ganglia on the contralateral side (Cont-BG). First, the specimens were weighed to determine their wet weight. They were then placed in an oven at 105 °C and dried for 72 h. After drying, the specimens were weighed again to determine their dry weight. As described [20,21], the percentage of brain water content was derived by applying the following formula: (wet weight–dry weight)/wet weight $\times$ 100%.

2.12 Immunofluorescence Staining

On day 3 after ICH, samples were obtained, and paraffin-embedded slices were prepared according to the previously described method [17]. Brain slices were incubated with 5% BSA to block unspecific binding. After overnight incubation at 4 °C with primary antibodies—anti-Iba-1 (1:500, CST 17198, USA), anti-NeuN (1:500, Abcam, ab104224, UK) and anti-GFAP (1:500, CST, 3670)—procedures proceeded to subsequent steps. The samples were then incubated with fluorescence-conjugated secondary antibodies (Abcam, ab150115 and ab150077, UK) at room temperature for 2 h. After incubation with secondary antibodies, the cells were washed three times with PBS. Next, the nuclei were stained with DAPI (Abcam, ab228549, UK). Finally, the ImageJ software (1.54f, National Institutes of Health, Bethesda, MD, USA) was used to calculate and quantify the average number of positively stained cells.

2.13 Multiplex Immunohistochemical (mIHC)

Tissue sections were deparaffinized in xylene, rehydrated through a graded ethanol series, and rinsed with water. Antigen retrieval was performed by microwave heating in sodium citrate buffer (pH 6.0). Endogenous peroxidase activity was quenched with 3% H_2O_2 for 10 minutes. After washing with TBST, sections were blocked with 5% BSA for 30 minutes at room temperature. The sections were incubated with primary antibodies against VSIG4 (1:500, Abcam, ab252933, UK), TMEM119 (1:500, CST 90840, USA), and IBA1 (1:500, CST 17198, USA) for 1 hour at room temperature, followed by incubation with HRP-conjugated goat anti-rabbit secondary antibody

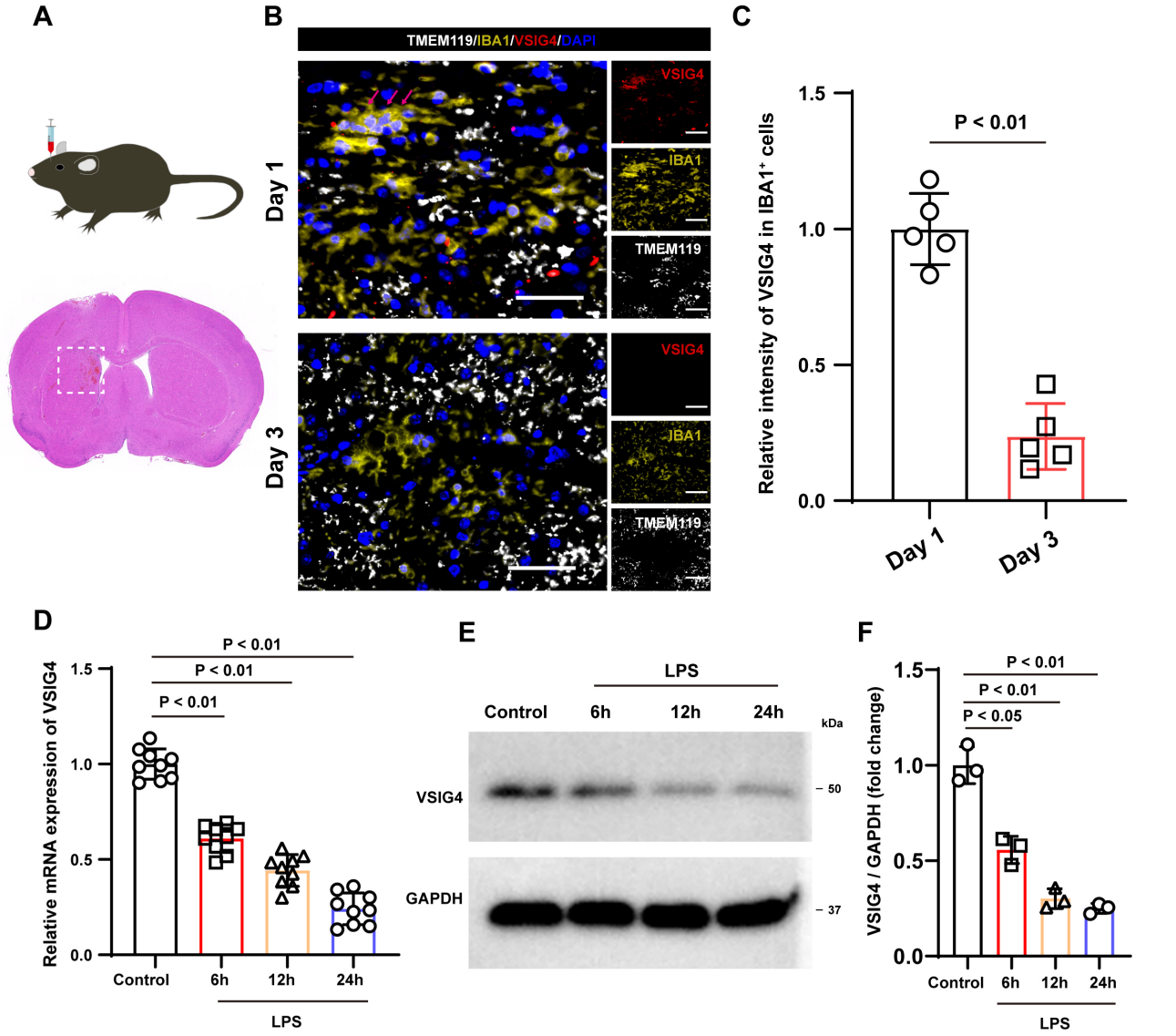

Fig. 1. Illustrates the expression characteristics of VSIG4 following ICH and the expression of VSIG4 in macrophages following LPS stimulation. (A) A schematic diagram outlining the experimental protocol carried out in mice. (B) Representative immunofluorescence images of VSIG4-positive cells, IBA1-positive cell and TMEM119-positive cells in the tissue surrounding the hematoma on days 1 and 3 after ICH, n = 5, scale 50 μm. The red arrow shows VSIG4^{+}IBA^{+}TMEM119^{-} cells. (C) The relative fluorescence intensity of VSIG4-positive and IBA1-positive cells in the tissue surrounding the hematoma on day 1 and day 3 after ICH, with n = 5. (D) The RT-qPCR results of VSIG4 mRNA in RAW264.7 cells after LPS stimulation. (E,F) Western blotting analysis of VSIG4 in RAW264.7 cells after LPS stimulation. VSIG4, V-set and immunoglobulin domain-containing 4; ICH, intracranial hemorrhage; LPS, lipopolysaccharide.

(absin, abs50012, Shanghai, China) for 10 minutes. Fluorescence signal amplification was achieved using tyramide conjugates (absin, abs50012, Shanghai, China) for 10 minutes. Nuclei were counterstained with DAPI (Abcam, ab228549, UK), and sections were mounted with anti-fade medium. Images were acquired using a fluorescence microscope (Olympus DP74, Olympus Corporation, Tokyo, Japan).

2.14 Hematoxylin and Eosin (HE) Staining

Brain tissues from each group of mice were collected and fixed in 4% paraformaldehyde at 4 °C for one week. Following paraffin embedding and sectioning, HE staining was performed according to the manufacturer's instructions (Solarbio, G1120, Beijing, China). Tissue sections were dehydrated using graded ethanol, and staining results were observed under an inverted fluorescence microscope (Olympus DP74, Olympus Corporation, Japan).

2.15 Statistical Analysis

Quantitative data are presented as mean ± SD. Intergroup differences were analyzed using Student's *t*-test (two groups) or one-way ANOVA with Tukey's post hoc analysis (multiple groups). Non-parametric data were evaluated via the Kruskal-Wallis test. Statistical significance was set at $p < 0.05$.

3. Results

3.1 The Expression of VSIG4 After ICH

Microglia and macrophages have similar functions and play essential roles in neuroinflammation after ICH [22]. It has been reported that VSIG4 can be expressed in peripheral macrophages [23]. To investigate VSIG4 expression in microglia/macrophages in brain tissue after ICH, we constructed an ICH mouse model and performed immunostaining (Fig. 1A). Immunostaining revealed VSIG4 expression exclusively in $IBA1^+$ $TMEM119^-$ cells (peripheral macrophages) post-ICH, with no detection in $IBA1^+$ $TMEM119^+$ microglia (Fig. 1B). In addition, compared to 1 day after ICH, the fluorescence intensity of VSIG4 in $IBA1^+$ cells decreased 3 days after ICH ($p < 0.01$), indicating that VSIG4 expression in macrophages after ICH was reduced, which is consistent with existing research (Fig. 1C) [24].

Inflammatory stimulation is an important factor that causes changes in macrophages. To examine VSIG4 expression in macrophages under inflammatory stimulation, RAW264.7 cells were treated with LPS (1 µg/mL) *in vitro*. RT-qPCR findings revealed that, compared to the control group, LPS treatment resulted in a time-dependent decrease in VSIG4 mRNA levels ($p < 0.01$) (Fig. 1D). Moreover, we measured VSIG4 protein levels, and found that the changes in VSIG4 protein levels following LPS stimulation were consistent with the changes in mRNA levels ($p < 0.01$) (Fig. 1E,F). These findings imply that upon exposure to an inflammatory stimulus, the VSIG4 expression level in macrophages progressively decreases.

3.2 VSIG4 Activates the Nuclear Factor Erythroid 2 Related Factor 2/Heme Oxygenase-1 (NRF2/HO-1) Pathway and Alleviates Oxidative Stress and Inflammatory Responses in Macrophages In Vitro

To explore the effects of VSIG4 on macrophages, we introduced recombinant VSIG4 (100 µg/mL) into RAW264.7 cells. Western blot analysis showed that VSIG4 treatment significantly upregulated the expression of NRF2 and HO-1 in RAW264.7 cells ($p < 0.05$), potentially affecting cellular antioxidant and stress response pathways (Fig. 2A–C). Prior research indicates that the NRF2/HO-1 axis modulates oxidative stress responses [25]. Therefore, we examined oxidative stress levels in macrophages. Compared to the IgG group, VSIG4 administration markedly elevated GSH levels and decreased SOD activity ($p < 0.01$) (Fig. 2D,E). Conversely, MDA levels notably decreased following VSIG4 intervention under LPS stimulation ($p < 0.01$) (Fig. 2F). These results indicate that VSIG4 can enhance the antioxidant capacity of cells, thereby effectively counteracting LPS-induced oxidative stress damage.

Oxidative stress has also been shown to activate inflammatory cells and release pro-inflammatory cytokines. As expected, ELISA findings demonstrated a notable increase in TNF-α and IL-1β levels in macrophages treated with LPS. In contrast, treatment with VSIG4 resulted in a notable decrease in TNF-α and IL-1β levels compared to the IgG group ($p < 0.01$) (Fig. 2G,H). This suggests that VSIG4 plays a key role in inhibiting excessive inflammatory responses during inflammatory induction. Collectively, these findings indicate that VSIG4 activates the NRF2/HO-1 pathway, thereby inhibiting oxidative stress and inflammatory responses in macrophages.

Subsequently, we conducted a co-culture experiment with HT22 and RAW264.7 cells treated with various treatments to investigate the potential protective effect of VSIG4-induced macrophages *in vitro*. According to the CCK-8 assay results, no significant difference was observed in cell viability between the two groups without LPS exposure. However, under LPS stimulation, VSIG4-treated RAW264.7 cells displayed improved viability compared to the IgG group ($p < 0.05$) (Fig. 2I). Bcl-2 and Bax are apoptosis-related proteins [26]. Western blot analysis showed that VSIG4-treated RAW264.7 cells partially reversed the changes in Bcl-2 and Bax expression levels under LPS stimulation ($p < 0.05$) (Fig. 2J–L). These findings revealed that VSIG4 helps preserve the equilibrium of anti-apoptotic signals, thereby protecting cells from LPS-induced damage and apoptosis.

3.3 VSIG4 Activates the NRF2/HO-1 Pathway and Alleviates ICH Injury In Vivo

Next, we evaluated the potential protective effects of VSIG4 in ICH mice. To this end, VSIG4 or IgG was injected into the mouse brain ventricle after ICH induction, and neurological function scoring was performed on day 3 after ICH. Parameters including cerebral edema severity, antioxidant/apoptotic protein expression, and inflammatory marker dynamics were further analyzed. Neurological function scores in the VSIG4 group showed significant improvement relative to the IgG controls ($p < 0.01$) (Fig. 3A). Further examination of brain water content revealed that VSIG4 markedly reduced brain tissue edema following ICH compared to the IgG group, indicating that it exerts a beneficial effect on the reduction of brain tissue damage and swelling ($p < 0.01$) (Fig. 3B). Western blot analysis demonstrated that VSIG4 treatment markedly elevated NRF2 and HO-1 protein levels in brain tissue ($p < 0.01$). Furthermore, VSIG4 therapy significantly upregulated Bcl-2 expression and reduced Bax expression (Bcl-2, $p < 0.01$; Bax, $p < 0.05$) (Fig. 3C–G).

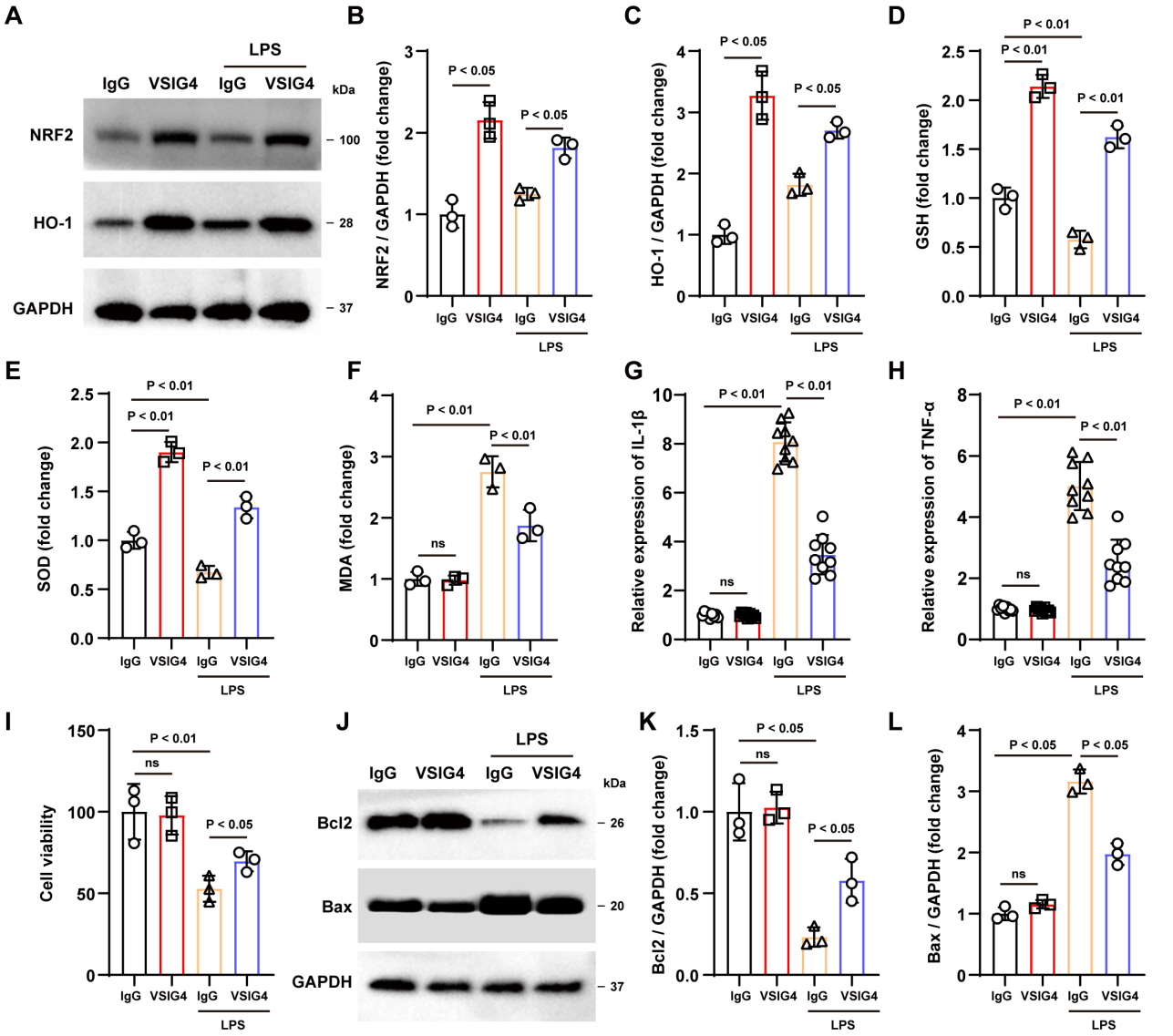

Fig. 2. Recombinant VSIG4 activates the NRF2 signaling pathway to inhibit oxidative stress and inflammatory responses in macrophages. (A–C) Western blotting analysis of NRF2 and HO-1 in RAW264.7 cells after the addition of recombinant VSIG4, n = 3. (D–F) Levels of GSH, SOD, and MDA in RAW264.7 cells after the addition of recombinant VSIG4, n = 3. (G,H) Levels of IL-1β and TNF-α in RAW264.7 cells after the addition of recombinant VSIG4, n = 9. (I) Survival of HT22 cells after co-culture with RAW264.7 cells treated with different treatments. (J–L) Western blot analyses were performed to examine Bcl-2 and Bax in HT22 cells following co-culture with RAW264.7 cells exposed to different treatments, n = 3. NRF2, nuclear factor erythroid 2 related factor 2; HO-1, heme oxygenase-1; GSH, glutathione; SOD, superoxide dismutase; MDA, malondialdehyde; IL-1β, interleukin-1β; TNF-α, tumor necrosis factor-alpha; Bcl-2, B-cell lymphoma 2. "ns" means no significant difference.

Correspondingly, analysis of antioxidant indicators showed that VSIG4 treatment significantly increased GSH and SOD levels in brain tissue (GSH, $p < 0.05$; SOD, $p < 0.01$) (Fig. 3H,I), while MDA levels significantly decreased ($p < 0.01$) (Fig. 3J). Moreover, VSIG4 significantly reduced the expression of the pro-inflammatory cytokines IL-1β and TNF-α in brain tissue ($p < 0.01$) (Fig. 3K,L).

Additionally, we observed that VSIG4 therapy reduced Iba-1$^+$ and GFAP$^+$ cell counts while increasing the NeuN$^+$ cell population in mouse brain tissue compared to the IgG group ($p < 0.01$) (Fig. 4A–F). These results confirm that VSIG4 also has an anti-oxidative stress effect and inhibits inflammatory responses *in vivo*, thereby providing favorable conditions for improving neurological function and promoting tissue repair.

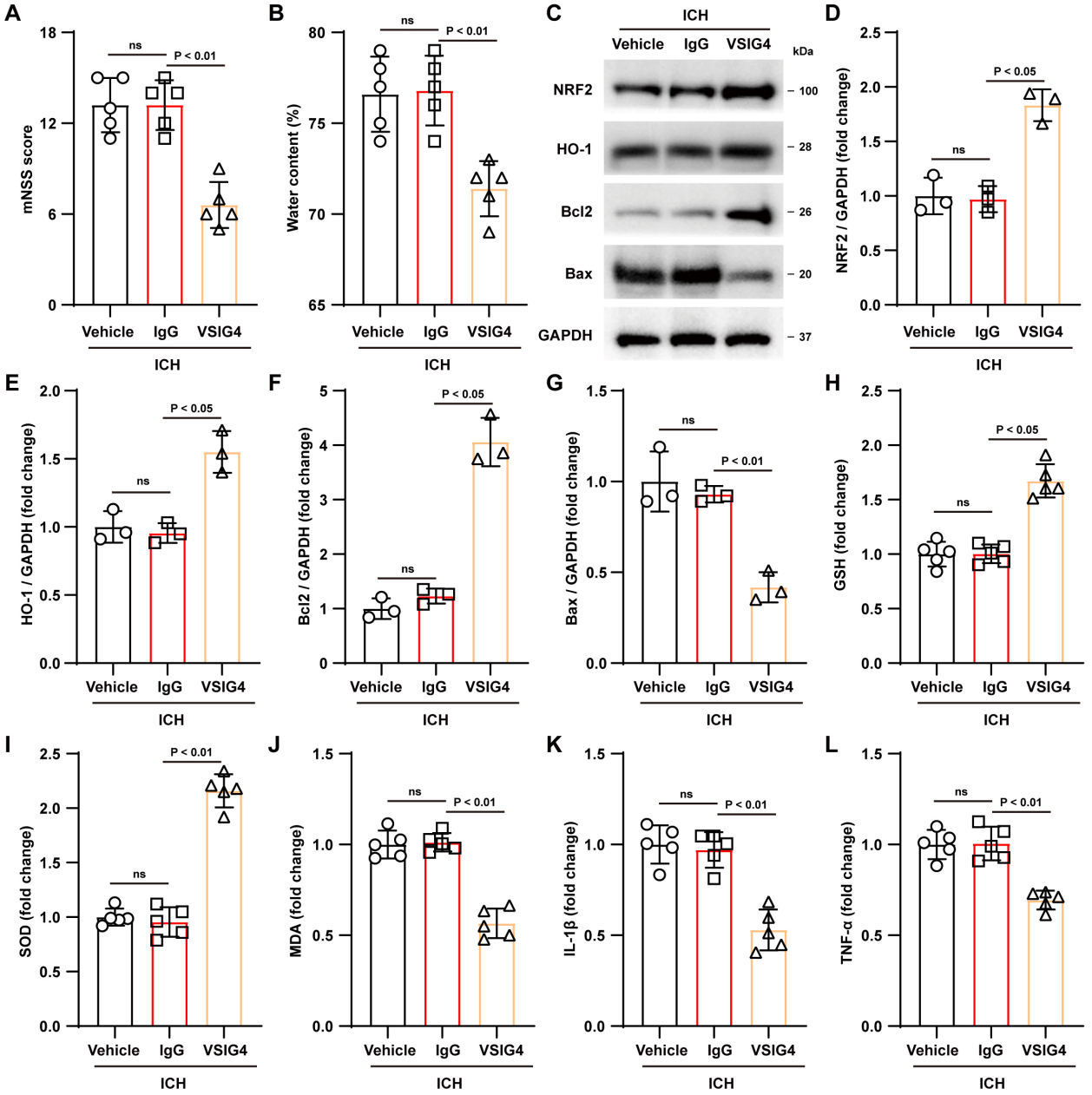

Fig. 3. Effect of VSIG4 on ICH mouse outcomes. (A) Neurological scores, n = 5. (B) Brain water content, n = 5. (C–G) Western blot assays were conducted in ICH mice to examine NRF2, HO-1, Bcl-2, and Bax, n = 3. (H–L) Levels of GSH, SOD, MDA, and the pro-inflammatory factors IL-1β and TNF-α measured in ICH mice, n = 5. "ns" means no significant difference.

3.4 VSIG4 Attenuates Macrophage Oxidative Stress and Inflammatory Responses Through NRF2/HO-1 Signaling In Vitro

To verify whether VSIG4 alleviates oxidative stress and inflammatory responses in macrophages *in vitro* through the NRF2/HO-1 pathway, we treated RAW264.7 cells with the NRF2 inhibitor brusatol [27]. Western blot results showed that brusatol reduced NRF2 and HO-1 expression and inhibited VSIG4-induced upregulation of NRF2 and HO-1 expression ($p < 0.05$) (Fig. 5A–C). Compared to VSIG4 treatment alone, VSIG4 and brusatol co-treatment resulted in lower GSH and SOD levels and higher MDA levels in RAW264.7 cells ($p < 0.05$) (Fig. 5D–F). ELISA results also suggested that brusatol increased IL-1β and TNF-α production ($p < 0.01$) (Fig. 5G,H). Our data indicated that brusatol treatment abrogated the inhibitory effects of VSIG4 on oxidative stress and inflammatory responses following LPS stimulation.

Subsequently, we co-cultured brusatol-treated RAW264.7 cells with HT22 cells to determine whether VSIG4 confers a protective effect on neurons through the NRF2/HO-1 signaling pathway. As shown in Fig. 5I,

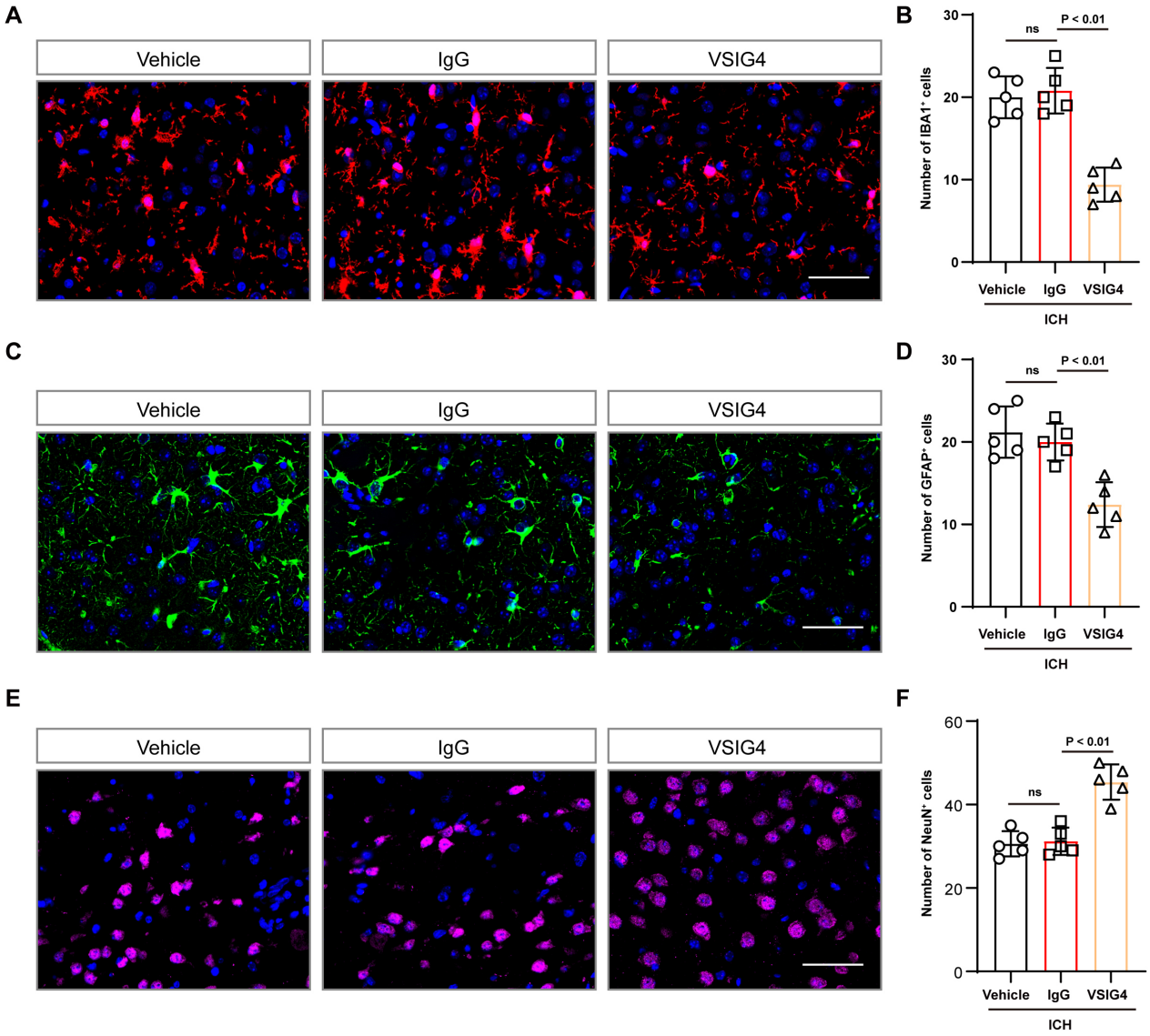

Fig. 4. Effect of VSIG4 on IBA1-positive cells and GFAP-positive cells in ICH mice. (A,B) Representative immunofluorescence images and cell numbers of IBA1-positive cells in the tissue surrounding the hematoma after ICH, n = 5, scale 50 µm. (C,D) Illustrative immunofluorescence images and corresponding cell counts of GFAP-positive cells in the tissue surrounding the hematoma after ICH, n = 5, scale 50 µm. (E,F) Illustrative immunofluorescence images and corresponding cell counts of NeuN-positive cells in the tissue surrounding the hematoma after ICH, n = 5, scale 50 µm. "ns" means no significant difference.

brusatol treatment reduced the survival rate of LPS-treated HT22 cells ($p < 0.01$). However, the combination of brusatol and VSIG4 downregulated Bcl-2 levels but had no significant effect on Bax levels ($p < 0.05$) (Fig. 5J–L). These results indicate that brusatol application impaired the neuroprotective ability of VSIG4-treated macrophages under LPS stimulation.

3.5 VSIG4 Alleviates ICH Injury via the NRF2/HO-1 Pathway In Vivo

To further elucidate the protective effect of VSIG4 in the ICH model and its relationship with the NRF2/HO-1 pathway, we conducted a comparative analysis of neurological function, histopathological changes, and molecular-level changes between the VSIG4-only treatment group and the brusatol intervention group following ICH.

The results demonstrated that brusatol administration, which inhibits NRF2 signaling, worsened the neurological deficits in ICH mice, increased brain tissue water content ($p < 0.05$), and significantly weakened the beneficial effects of VSIG4 on neurological function recovery and cerebral edema reduction ($p < 0.01$) (Fig. 6A,B). These results indicate that NRF2 plays a pivotal role in regulating the protective effects of VSIG4.

Consistent with the *in vitro* findings, brusatol administration resulted in a significant reduction in the increased

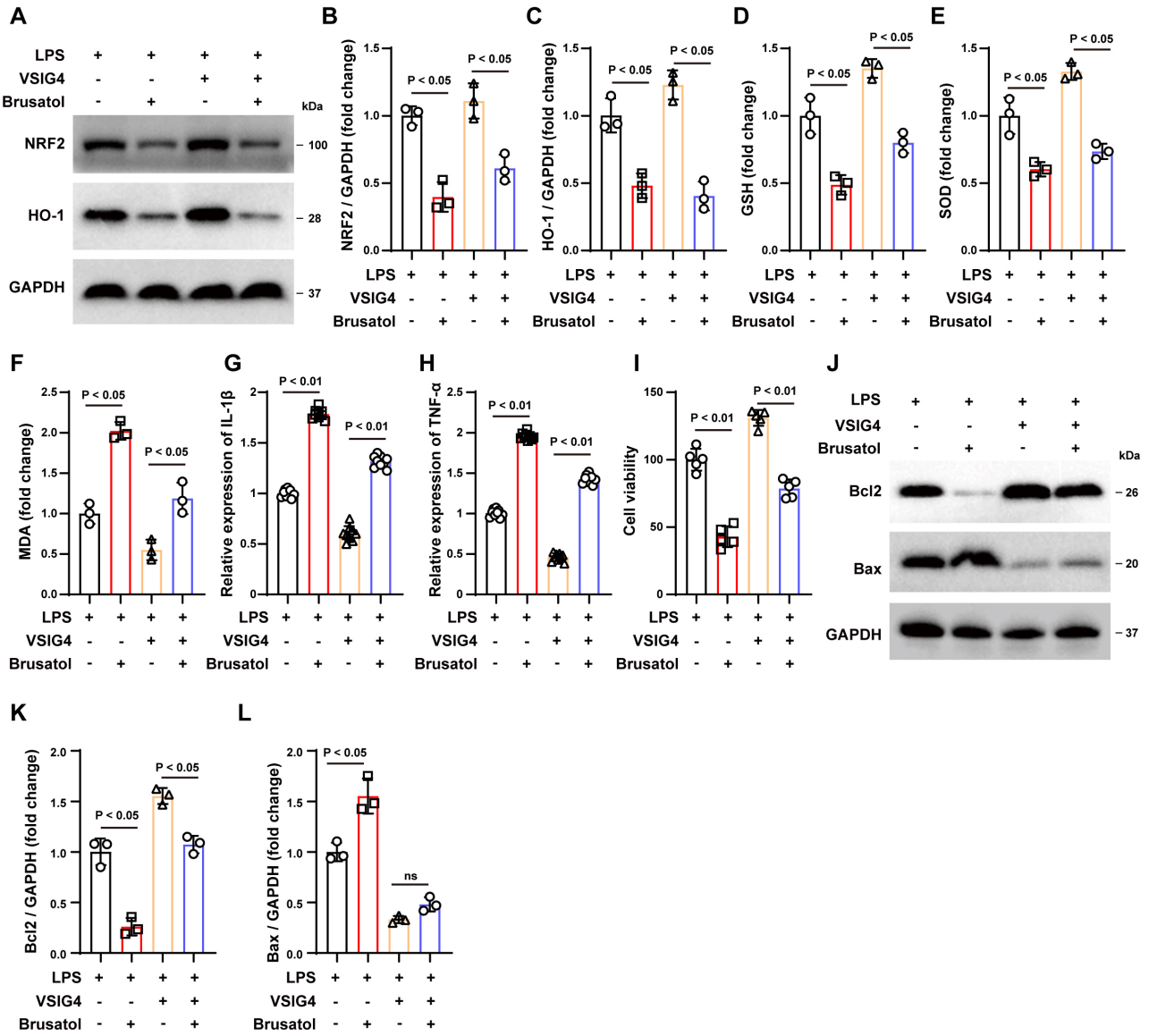

Fig. 5. The NRF2 inhibitor Brusatol inhibits the protective effect of VSIG4 *in vitro*. (A–C) Western blotting analysis of NRF2 and HO-1 in RAW264.7 cells exposed to Brusatol, n = 3. (D–F) Levels of GSH, SOD and MDA levels in Brusatol-exposed RAW264.7 cells, n = 3. (G,H) Concentrations of IL-1β and TNF-α in RAW264.7 cells treated with Brusatol, n = 9. (I) Survival of HT22 cells after co-culture with RAW264.7 cells treated with different treatments. (J–L) Western blot analysis was performed to detect Bcl-2 and Bax protein expression in HT22 cells following co-culture with RAW264.7 cells subjected to various treatments, n = 3. "ns" means no significant difference.

expression of NRF2 ($p < 0.05$) and HO-1 ($p < 0.05$) in brain tissue after VSIG4 treatment (Fig. 6C–E). Detection of apoptosis-related proteins revealed that adding brusatol alone significantly reduced Bcl-2 expression levels ($p < 0.05$) and significantly increased Bax expression levels ($p < 0.05$). The VSIG4 group demonstrated the capacity to upregulate Bcl-2 and downregulate Bax, thereby reducing apoptosis. However, the addition of brusatol significantly weakened this protective effect ($p < 0.05$) (Fig. 6F,G). Among the antioxidant markers, VSIG4 treatment resulted in a significant increase in GSH and SOD levels and a reduction in MDA content. However, the improvement in these antioxidant markers was impaired after inhibition of the NRF2 pathway ($p < 0.01$) (Fig. 6H–J).

Tissue immunofluorescence staining and cell counting demonstrated that VSIG4 markedly diminished the aberrant proliferation of IBA1$^+$ and GFAP$^+$ cells, thereby attenuating the pro-inflammatory response and increasing NeuN$^+$ cells survival. Conversely, brusatol increased the number of inflammatory cells ($p < 0.05$) and reduced NeuN$^+$ cells survival ($p < 0.01$) (Fig. 6K–M, **Supplementary Fig. 1A–C**). The results of the inflammatory factor detection were

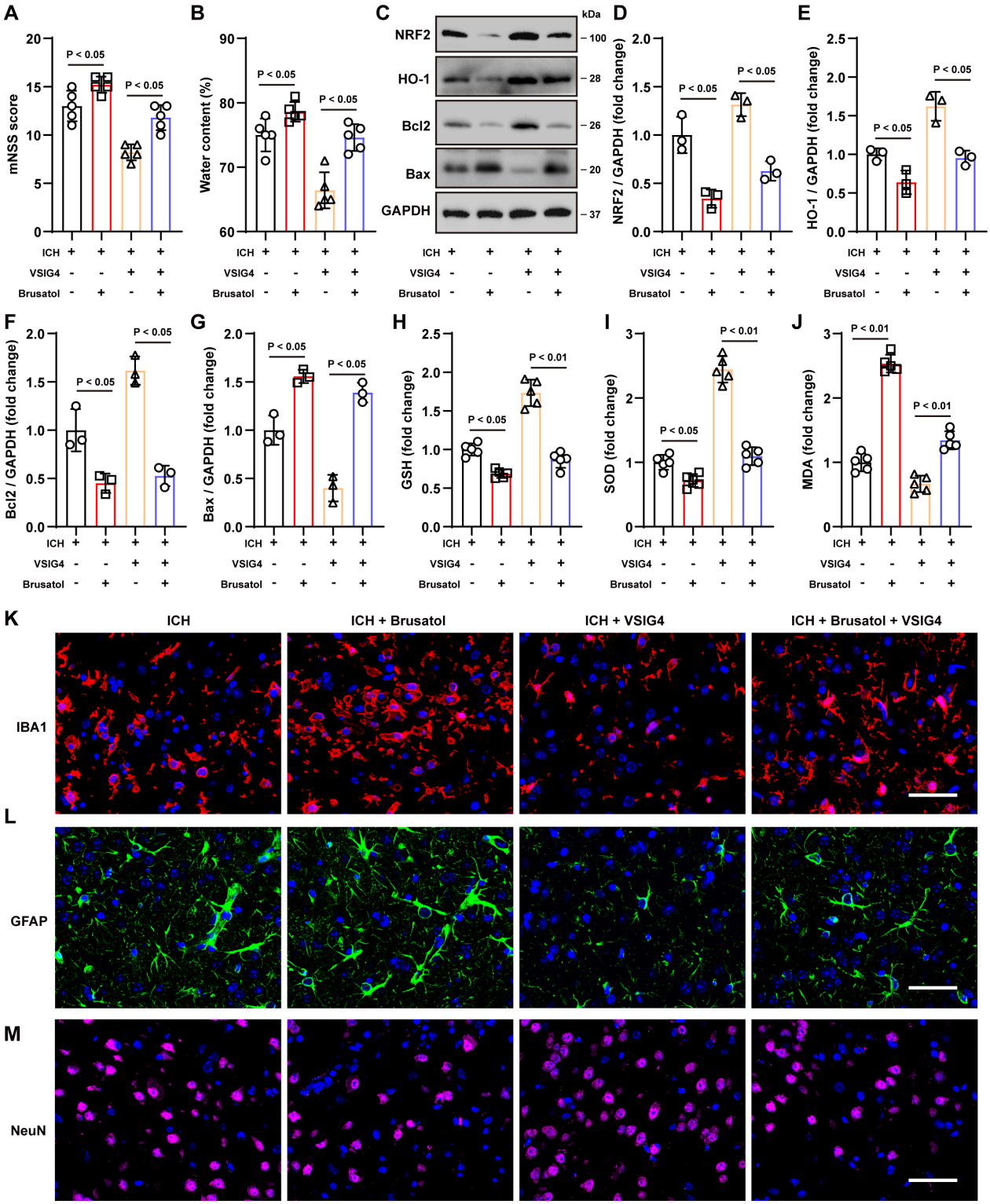

Fig. 6. The NRF2 inhibitor Brusatol inhibits the protective effect of VSIG4 *in vivo*. (A) Neurological scores, n = 5. (B) Brain water content, n = 5. (C–G) Western blot analysis was conducted to measure the protein levels of NRF2, HO-1, Bcl-2, and Bax in brain tissues from ICH mice treated with Brusatol, n = 3. (H–J) Levels of GSH, SOD and MDA levels in ICH mice exposed to Brusatol, n = 5. (K–M) Representative immunofluorescence images and quantification of cells positive for IBA1, GFAP, and NeuN in the perihematomal region following Brusatol treatment, n = 5, scale 50 μm. "ns" means no significant difference.

also consistent with this conclusion. VSIG4 inhibited the overexpression of IL-1β and TNF-α following ICH. However, this inhibitory effect was significantly weakened following brusatol treatment ($p < 0.01$) (**Supplementary Fig. 1D,E**).

In conclusion, VSIG4 exerts notable neuroprotective effects *in vivo* by upregulating the NRF2/HO-1 pathway. These effects include improving neurological function, reducing cerebral edema, inhibiting apoptosis and oxidative stress, and suppressing excessive inflammatory responses. However, adding the NRF2 inhibitor brusatol significantly diminished the protective effects of VSIG4.

4. Discussion

Intracranial hemorrhage is linked to high rates of fatality and disability and represents a serious threat to human health. Its pathophysiological mechanisms include both direct and secondary damage. To date, intracerebral hematoma removal remains the central clinical intervention for patients with ICH and can help reduce mortality and prevent further neurological deterioration. However, studies investigating the long-term functional recovery benefits of surgical intervention have yielded inconsistent results and currently lack robust, high-quality evidence [28]. These inconsistencies may stem from the difficulty of hematoma removal, surgeon expertise, and treatment time window. Therefore, targeting secondary damage after ICH, such as oxidative stress and neuroinflammation, is a potential treatment strategy for functional recovery.

This study comprehensively investigated the alterations and therapeutic effects associated with VSIG4 in ICH and LPS stimulation models and explored the underlying mechanisms in detail. Our findings indicate that VSIG4 has a neuroprotective effect. Microglia are generally considered prominent participants in the immune reaction of the central nervous system [29]. Unlike previous study [18], we found that VSIG4 was mainly expressed in macrophages rather than microglia. In addition, our data showed that VSIG4 expression decreased as ICH duration increased, suggesting a negative correlation between VSIG4 expression levels and ICH severity, providing insight into the function of VSIG4. After exogenous VSIG4 intervention, we found that VSIG4 upregulated the expression of a series of anti-oxidative enzymes, such as HO-1 and SOD, decreased levels of substances, such as GSH, and reduced the production of oxidative damage markers, such as MDA [30]. These changes effectively relieved oxidative stress and inflammatory damage in brain tissue and cells subjected to ICH and LPS stimulation, thereby increasing HT22 cell survival rate, improving neurological function, and reducing cerebral edema. Furthermore, VSIG4 upregulated Bcl-2 and reduced Bax expression, which supports its positive role in apoptosis regulation [31]. Bcl-2 functions as an anti-apoptotic protein, preventing the formation of holes in the outer mitochondrial membrane. However, Bcl-2 activity is inhibited by binding to Bax, which can damage cell integrity, release apoptotic factors, and initiate an apoptotic cascade [32,33]. A high Bcl-2/Bax ratio inhibits the mitochondrial apoptotic pathway, prevents cytochrome C escape from mitochondria, enables caspase-9 and caspase-3 activation, and promotes cell survival. Additionally, VSIG4's inhibitory effect on microglial and astrocyte activation in an inflammatory environment further underscores its importance in maintaining the balance of the neural microenvironment. By decreasing the secretion of pro-inflammatory mediators, including IL-1β and TNF-α, and reducing the number of activated inflammatory cells [34,35], VSIG4 can alleviate the secondary damage to brain tissue caused by the inflammatory cascade. These findings align with emerging evidence on CNS inflammation modulators [36,37], positioning VSIG4 as a potential therapeutic candidate for cerebrovascular injuries and neuroinflammatory disorders.

Second, our study clarified that VSIG4 exerts its protective effects by regulating the NRF2/HO-1 signaling pathway. NRF2 is considered a key transcription factor in cells responding to oxidative stress and inflammatory responses. Under physiological conditions, NRF2 is bound to Keap1, retained in the cytoplasm, and steadily degraded via the ubiquitin-proteasome pathway [38]. However, under stress conditions, NRF2 is released and transferred to the nucleus, promoting the expression of antioxidant genes, including HO-1 [25]. HO-1 can achieve antioxidant effects by promoting heme degradation and inhibiting signaling pathways such as NF-κB and MAPK [39,40]. In addition, the NRF2/HO-1 pathway has been shown to directly or indirectly increase the Bcl-2/Bax ratio, thereby inhibiting apoptosis [41,42]. One study indicated that VSIG4 overexpression increased NRF2 expression and that VSIG4 was co-expressed with Keap1 in a co-immunoprecipitation experiment [15]. Our study also showed that as VSIG4 levels increased, NRF2 and HO-1 expression levels increased accordingly. However, after brusatol inhibited NRF2 signaling, the neuroprotective, antioxidant, and anti-inflammatory effects of VSIG4 were significantly attenuated. The interaction between VSIG4 and Keap1 could be a possible mechanism by which VSIG4 activates the NRF2/HO-1 pathway; however, we were unable to investigate this further.

Moreover, the present study has certain limitations. For instance, the study was exclusively verified in a mouse model, and there are significant differences in pathophysiology between humans and mice, including differences in hematoma size, inflammation duration, and immune cell infiltration pattern. Furthermore, human patients with ICH exhibit larger hematoma volumes, which consequently extend the time window for the inflammatory response. Additionally, VSIG4 and NRF2 signaling pathway activation may undergo distinct dynamic changes. There are also differences in the response patterns of immune cells, such

as macrophages and microglia, between humans and mice. Although the protective role of VSIG4 has been confirmed in animal experiments, further exploration is necessary to assess its feasibility in clinical settings, determine the optimal administration route, and evaluate potential safety concerns.

5. Conclusions

The current study provides experimental evidence for the neuroprotective mechanism of VSIG4 in ICH. VSIG4 improves neurological deficits and mitigates tissue damage after ICH by activating the NRF2/HO-1 pathway, enhancing antioxidant capacity, and inhibiting excessive inflammatory responses. Future studies should focus on elucidating the molecular mechanism underlying the interaction between VSIG4 and NRF2 and evaluating its potential value in clinical applications.

Availability of Data and Materials

The data that support the findings of this study are available from the corresponding authors upon reasonable request.

Author Contributions

SQ and LZ were responsible for experimental design and project management. HL and YL conducted experimental procedures and data analysis. HL drafted the initial manuscript and participated in revisions, while YL prepared the figures/charts and contributed to manuscript editing. YZ and WQ assisted in figure/chart preparation and manuscript revisions. ZS participated in experimental design and manuscript polishing. All authors contributed to editorial changes in the manuscript. All authors read and approved the final manuscript. All authors have participated sufficiently in the work and agreed to be accountable for all aspects of the work.

Ethics Approval and Consent to Participate

For mice, all experimental protocols followed the ARRIVE guidelines and were approved by the Laboratory Animal Management and Ethics Committee of Huzhou Central Hospital (Approval number: 202411005).

Acknowledgment

We would like to express our gratitude to all those who helped us during the writing of this manuscript.

Funding

This work was supported by the Shenzhen Natural Science Fund (No. JCYJ20210324134800001 and JCYJ20190808103401655 to Lifang Zheng), the Huzhou City Public Welfare Applied Research Project (No. 2022GZ63 to Sheng Qiu) and the Zhejiang Chinese Medical University Affiliated Hospital Scientific Research Project (No. 2023FSYYZZ16 to Sheng Qiu).

Conflict of Interest

The authors declare no conflict of interest.

Declaration of AI and AI-assisted Technologies in the Writing Process

During the preparation of this work the authors used Grammarly in order to check spell and grammar. After using this tool, the authors reviewed and edited the content as needed and takes full responsibility for the content of the publication.

Supplementary Material

Supplementary material associated with this article can be found, in the online version, at https://doi.org/10.31083/FBL37810.

References

[1] GBD 2021 Stroke Risk Factor Collaborators. Global, regional, and national burden of stroke and its risk factors, 1990-2021: a systematic analysis for the Global Burden of Disease Study 2021. The Lancet. Neurology. 2024; 23: 973–1003. https://doi.org/10.1016/S1474-4422(24)00369-7.

[2] Magid-Bernstein J, Girard R, Polster S, Srinath A, Romanos S, Awad IA, *et al*. Cerebral Hemorrhage: Pathophysiology, Treatment, and Future Directions. Circulation Research. 2022; 130: 1204–1229. https://doi.org/10.1161/CIRCRESAHA.121.319949.

[3] Keep RF, Hua Y, Xi G. Intracerebral haemorrhage: mechanisms of injury and therapeutic targets. The Lancet. Neurology. 2012; 11: 720–731. https://doi.org/10.1016/S1474-4422(12)70104-7.

[4] Bautista W, Adelson PD, Bicher N, Themistocleous M, Tsivgoulis G, Chang JJ. Secondary mechanisms of injury and viable pathophysiological targets in intracerebral hemorrhage. Therapeutic Advances in Neurological Disorders. 2021; 14: 17562864211049208. https://doi.org/10.1177/17562864211049208.

[5] Shao L, Chen S, Ma L. Secondary Brain Injury by Oxidative Stress After Cerebral Hemorrhage: Recent Advances. Frontiers in Cellular Neuroscience. 2022; 16: 853589. https://doi.org/10.3389/fncel.2022.853589.

[6] Kearns KN, Ironside N, Park MS, Worrall BB, Southerland AM, Chen CJ, *et al*. Neuroprotective Therapies for Spontaneous Intracerebral Hemorrhage. Neurocritical Care. 2021; 35: 862–886. https://doi.org/10.1007/s12028-021-01311-3.

[7] Liu B, Cheng L, Gao H, Zhang J, Dong Y, Gao W, *et al*. The biology of VSIG4: Implications for the treatment of immune-mediated inflammatory diseases and cancer. Cancer Letters. 2023; 553: 215996. https://doi.org/10.1016/j.canlet.2022.215996.

[8] Vogt L, Schmitz N, Kurrer MO, Bauer M, Hinton HI, Behnke S, *et al*. VSIG4, a B7 family-related protein, is a negative regulator of T cell activation. The Journal of Clinical Investigation. 2006; 116: 2817–2826. https://doi.org/10.1172/JCI25673.

[9] Huang X, Feng Z, Jiang Y, Li J, Xiang Q, Guo S, *et al*. VSIG4 mediates transcriptional inhibition of *Nlrp3* and *Il-1β* in macrophages. Science Advances. 2019; 5: eaau7426. https://doi.org/10.1126/sciadv.aau7426.

[10] Li J, Diao B, Guo S, Huang X, Yang C, Feng Z, *et al*. VSIG4 inhibits proinflammatory macrophage activation by reprogramming mitochondrial pyruvate metabolism. Nature Communications. 2017; 8: 1322. https://doi.org/10.1038/s41467-017-01327-4.

[11] Liao Y, Deng C, Wang X. VSIG4 ameliorates intestinal inflammation through inhibiting macrophages NLRP3 inflammasome and pyroptosis. Tissue & Cell. 2024; 86: 102285. https://doi.org/10.1016/j.tice.2023.102285.

[12] Wang Y, Zhang Y, Li J, Li C, Zhao R, Shen C, *et al*. Hypoxia Induces M2 Macrophages to Express VSIG4 and Mediate Cardiac Fibrosis After Myocardial Infarction. Theranostics. 2023; 13: 2192–2209. https://doi.org/10.7150/thno.78736.

[13] Cai P, Wang J, Xu J, Zhang M, Yin X, He S, *et al*. V-set and immunoglobulin domain containing 4 inhibits oxidative stress, mitochondrial dysfunction, and inflammation to attenuate Parkinson's disease progression by activating the JAK2/STAT3 pathway. Journal of Neuroimmunology. 2024; 391: 578345. https://doi.org/10.1016/j.jneuroim.2024.578345.

[14] Lyu Q, Pang X, Zhang Z, Wei Y, Hong J, Chen H. Microglial V-set and immunoglobulin domain-containing 4 protects against ischemic stroke in mice by suppressing TLR4-regulated inflammatory response. Biochemical and Biophysical Research Communications. 2020; 522: 560–567. https://doi.org/10.1016/j.bbrc.2019.11.077.

[15] Miao J, Tu Y, Jiang J, Ren R, Wu Q, Liang H, *et al*. VSIG4 inhibits RANKL-induced osteoclastogenesis by enhancing Nrf2-dependent antioxidant response against reactive oxygen species production. International Journal of Biological Macromolecules. 2024; 260: 129357. https://doi.org/10.1016/j.ijbiomac.2024.129357.

[16] Xu Y, Ma HY, Qiao CY, Peng Y, Ding Q, Xiang RL, *et al*. Significance of changes in the concentration of inflammatory factors in blood or cerebrospinal fluid in evaluating the severity and prognosis of spontaneous cerebral hemorrhage: A systematic review and meta-analysis. Clinical Neurology and Neurosurgery. 2021; 205: 106631. https://doi.org/10.1016/j.clineuro.2021.106631.

[17] Chen S, Li L, Peng C, Bian C, Ocak PE, Zhang JH, *et al*. Targeting Oxidative Stress and Inflammatory Response for Blood-Brain Barrier Protection in Intracerebral Hemorrhage. Antioxidants & Redox Signaling. 2022; 37: 115–134. https://doi.org/10.1089/ars.2021.0072.

[18] Zhang D, Shen X, Pang K, Yang Z, Yu A. VSIG4 alleviates intracerebral hemorrhage induced brain injury by suppressing TLR4-regulated inflammatory response. Brain Research Bulletin. 2021; 176: 67–75. https://doi.org/10.1016/j.brainresbull.2021.08.008.

[19] Chen J, Sanberg PR, Li Y, Wang L, Lu M, Willing AE, *et al*. Intravenous administration of human umbilical cord blood reduces behavioral deficits after stroke in rats. Stroke. 2001; 32: 2682–2688. https://doi.org/10.1161/hs1101.098367.

[20] Ye XH, Xu ZM, Shen D, Jin YJ, Li JW, Xu XH, *et al*. Gas6/Axl signaling promotes hematoma resolution and motivates protective microglial responses after intracerebral hemorrhage in mice. Experimental Neurology. 2024; 382: 114964. https://doi.org/10.1016/j.expneurol.2024.114964.

[21] Marmarou A, Foda MA, van den Brink W, Campbell J, Kita H, Demetriadou K. A new model of diffuse brain injury in rats. Part I: Pathophysiology and biomechanics. Journal of Neurosurgery. 1994; 80: 291–300. https://doi.org/10.3171/jns.1994.80.2.0291.

[22] Hu X, Li P, Guo Y, Wang H, Leak RK, Chen S, *et al*. Microglia/macrophage polarization dynamics reveal novel mechanism of injury expansion after focal cerebral ischemia. Stroke. 2012; 43: 3063–3070. https://doi.org/10.1161/STROKEAHA.112.659656.

[23] He JQ, Wiesmann C, van Lookeren Campagne M. A role of macrophage complement receptor CRIg in immune clearance and inflammation. Molecular Immunology. 2008; 45: 4041–4047. https://doi.org/10.1016/j.molimm.2008.07.011.

[24] Ji N, Wu L, Shi H, Li Q, Yu A, Yang Z. VSIG4 Attenuates NLRP3 and Ameliorates Neuroinflammation via JAK2-STAT3-A20 Pathway after Intracerebral Hemorrhage in Mice. Neurotoxicity Research. 2022; 40: 78–88. https://doi.org/10.1007/s12640-021-00456-5.

[25] Loboda A, Damulewicz M, Pyza E, Jozkowicz A, Dulak J. Role of Nrf2/HO-1 system in development, oxidative stress response and diseases: an evolutionarily conserved mechanism. Cellular and Molecular Life Sciences: CMLS. 2016; 73: 3221–3247. https://doi.org/10.1007/s00018-016-2223-0.

[26] Wang F, Zhang C, Zhang Q, Li J, Xue Y, He X, *et al*. Lithium ameliorates spinal cord injury through endoplasmic reticulum stress-regulated autophagy and alleviated apoptosis through IRE1 and PERK/eIF2α signaling pathways. Journal of Neurorestoratology. 2023; 11: 100081. https://doi.org/10.1016/j.jnrt.2023.100081.

[27] Ren D, Villeneuve NF, Jiang T, Wu T, Lau A, Toppin HA, *et al*. Brusatol enhances the efficacy of chemotherapy by inhibiting the Nrf2-mediated defense mechanism. Proceedings of the National Academy of Sciences of the United States of America. 2011; 108: 1433–1438. https://doi.org/10.1073/pnas.1014275108.

[28] Greenberg SM, Ziai WC, Cordonnier C, Dowlatshahi D, Francis B, Goldstein JN, *et al*. 2022 Guideline for the Management of Patients With Spontaneous Intracerebral Hemorrhage: A Guideline From the American Heart Association/American Stroke Association. Stroke. 2022; 53: e282–e361. https://doi.org/10.1161/STR.0000000000000407.

[29] Woodburn SC, Bollinger JL, Wohleb ES. The semantics of microglia activation: neuroinflammation, homeostasis, and stress. Journal of Neuroinflammation. 2021; 18: 258. https://doi.org/10.1186/s12974-021-02309-6.

[30] Jomova K, Alomar SY, Alwasel SH, Nepovimova E, Kuca K, Valko M. Several lines of antioxidant defense against oxidative stress: antioxidant enzymes, nanomaterials with multiple enzyme-mimicking activities, and low-molecular-weight antioxidants. Archives of Toxicology. 2024; 98: 1323–1367. https://doi.org/10.1007/s00204-024-03696-4.

[31] Wang Y, Tian M, Tan J, Pei X, Lu C, Xin Y, *et al*. Irisin ameliorates neuroinflammation and neuronal apoptosis through integrin αVβ5/AMPK signaling pathway after intracerebral hemorrhage in mice. Journal of Neuroinflammation. 2022; 19: 82. https://doi.org/10.1186/s12974-022-02438-6.

[32] Murphy KM, Ranganathan V, Farnsworth ML, Kavallaris M, Lock RB. Bcl-2 inhibits Bax translocation from cytosol to mitochondria during drug-induced apoptosis of human tumor cells. Cell Death and Differentiation. 2000; 7: 102–111. https://doi.org/10.1038/sj.cdd.4400597.

[33] Dewson G, Kluck RM. Mechanisms by which Bak and Bax permeabilise mitochondria during apoptosis. Journal of Cell Science. 2009; 122: 2801–2808. https://doi.org/10.1242/jcs.038166.

[34] Gheorghe RO, Deftu A, Filippi A, Grosu A, Bica-Popi M, Chiritoiu M, *et al*. Silencing the Cytoskeleton Protein Iba1 (Ionized Calcium Binding Adapter Protein 1) Interferes with BV2 Microglia Functioning. Cellular and Molecular Neurobiology. 2020; 40: 1011–1027. https://doi.org/10.1007/s10571-020-00790-w.

[35] Petrova ES, Kolos EA. Astrocyte Marker GFAP in Gliocytes of Peripheral Nervous System. Journal of Evolutionary Biochemistry and Physiology. 2024; 60: 1759–1771. https://doi.org/10.1134/S0022093024050090.

[36] Leal MC, Casabona JC, Puntel M, Pitossi FJ. Interleukin-1β and tumor necrosis factor-α: reliable targets for protective therapies in Parkinson's Disease? Frontiers in Cellular Neuroscience. 2013; 7: 53. https://doi.org/10.3389/fncel.2013.00053.

[37] Wang RPH, Huang J, Chan KWY, Leung WK, Goto T, Ho

YS, *et al*. IL-1β and TNF-α play an important role in modulating the risk of periodontitis and Alzheimer's disease. Journal of Neuroinflammation. 2023; 20: 71. https://doi.org/10.1186/s12974-023-02747-4.

[38] Zhang DD, Lo SC, Sun Z, Habib GM, Lieberman MW, Hannink M. Ubiquitination of Keap1, a BTB-Kelch substrate adaptor protein for Cul3, targets Keap1 for degradation by a proteasome-independent pathway. The Journal of Biological Chemistry. 2005; 280: 30091–30099. https://doi.org/10.1074/jbc.M501279200.

[39] Liu R, Zhang X, Nie L, Sun S, Liu J, Chen H. Heme oxygenase 1 in erythropoiesis: an important regulator beyond catalyzing heme catabolism. Annals of Hematology. 2023; 102: 1323–1332. https://doi.org/10.1007/s00277-023-05193-7.

[40] Ren J, Li L, Wang Y, Zhai J, Chen G, Hu K. Gambogic acid induces heme oxygenase-1 through Nrf2 signaling pathway and inhibits NF-κB and MAPK activation to reduce inflammation in LPS-activated RAW264.7 cells. Biomedicine & Pharmacotherapy. 2019; 109: 555–562. https://doi.org/10.1016/j.biopha.2018.10.112.

[41] Maher AM, Elsanosy GA, Ghareeb DA, Elblehi SS, Saleh SR. 10-Hydroxy Decanoic Acid and Zinc Oxide Nanoparticles Retrieve Nrf2/HO-1 and Caspase-3/Bax/Bcl-2 Signaling in Lead-Induced Testicular Toxicity. Biological Trace Element Research. 2024. https://doi.org/10.1007/s12011-024-04374-3. (online ahead of print)

[42] Gur C, Kandemir FM, Caglayan C, Satıcı E. Chemopreventive effects of hesperidin against paclitaxel-induced hepatotoxicity and nephrotoxicity via amendment of Nrf2/HO-1 and caspase-3/Bax/Bcl-2 signaling pathways. Chemico-biological Interactions. 2022; 365: 110073. https://doi.org/10.1016/j.cbi.2022.110073.